We sincerely appreciate the reviewers for taking the time to review our manuscript and for providing valuable comments. Based on the reviewers' suggestions, we have revised the paper. Below are our responses to each of the reviewers' comments, with the reviewers' comments in black, our responses in red, and the revised manuscript content in italicized orange font.

Reviewer 1

The authors considered the review comments by the previous reviewers in revising the manuscript. The manuscript is written reasonably well as a measurement report. I have a few concerns that will need to be addressed before the manuscript can be considered for publication.

We sincerely thank the reviewer for their valuable feedback, which has helped us improve the quality of our manuscript. In response to the reviewer's comments, we have added details regarding ACSM calibration, compared the data from ACSM and SMPS, and elaborated on the importance and novelty of the closure method.

The ACSM calibration

The authors mentioned that they calibrated the instrument for RIE. However, there is no descriptions about the IE calibration. Regarding the CE, it is typically needed to compare the AMS/ACSM data with the aerosol mass concentration for checking the validity of CE. The authors at least have the SMPS data. I wonder how the authors validate the estimated values of CE.

Reply: Thanks for the reviewer's valuable comment. We calibrated the ionization efficiency (IE) value of NO_3^- with the relative ionization efficiency (RIE) together. The calibration gives an IE value of 103.4 ions pg^{-1} and 98.9 ions pg^{-1} for nitrate in summer and winter cruises, respectively. We have included the information in lines 184-187:

The ionization efficiency (IE) and relative ionization efficiency (RIE) values of the instrument were calibrated using ammonium nitrate (NH_4NO_3) and ammonium sulfate ($(NH_4)_2SO_4$) both before the start and after the completion of the campaigns. The calibration gives an IE value of 103.4 ions pg^{-1} and 98.9 ions pg^{-1} for nitrate in summer and winter cruises, respectively.

In addition, we compared the ACSM data with SMPS measurements to verify the CE value. An average particle density of 1.5 g cm^{-3} was assumed to convert the PNSD data obtained from the SMPS into mass concentrations (Geller et al., 2006). Overall, the mass concentration time series measured by the ACSM and SMPS showed strong correlations, with correlation coefficients of 0.84 and 0.93 for summer and winter, respectively.

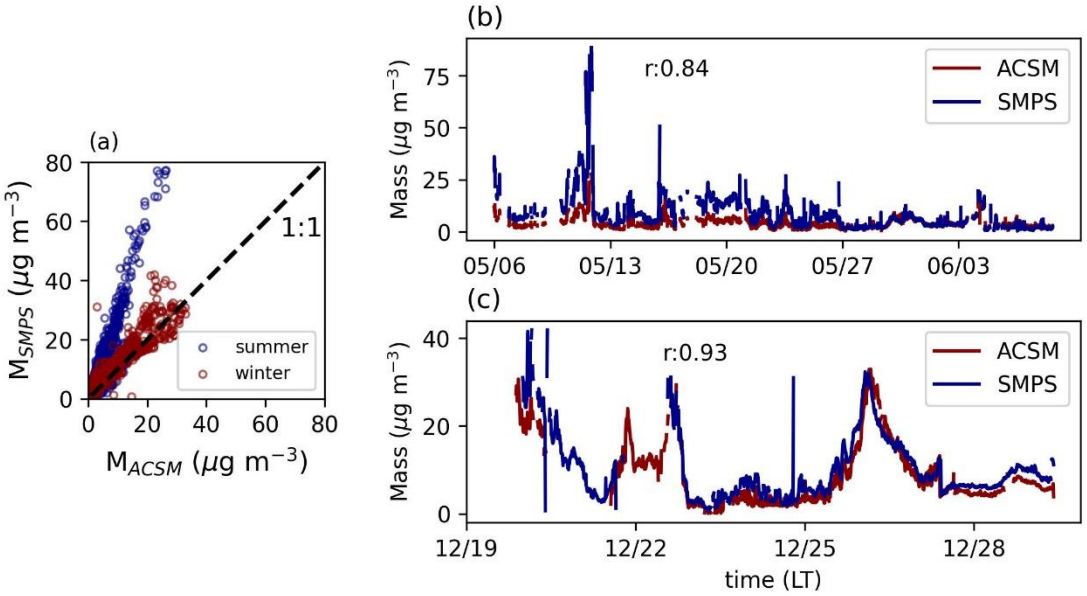

Figure S3. Comparison of mass concentration from ACSM and SMPS (a), the timeseries of mass concentration of ACSM and SMPS in summer (b), and the timeseries of mass concentration of ACSM and SMPS in winter (c).

However, before May 27 (prior to the onset of the summer monsoon), when air masses predominantly originating from Luzon in the Philippines were observed, SMPS-derived values consistently exceeded those measured by the ACSM. According to Chao et al. (2022), the summer monsoon onset occurred during the sixth pentad of May, which was approximately represented as May 27 for simplicity here. This discrepancy may be attributed to the ACSM's inability to detect certain refractory materials.

To further investigate this discrepancy, we compared black carbon concentrations during two distinct periods, utilizing measurements from the Aethalometer (Model AE33, Magee Scientific, USA). The differences in BC concentration between these periods were minor (0.67 μg m^{-3} vs 0.48 μg m^{-3}), insufficient to account for the observed discrepancy between the SMPS-derived mass concentration and ACSM mass concentration. It is noteworthy that the AE33 might underestimate BC concentrations during May 5 to 27, owing to the lower detection efficiency for smaller black carbon particles (< 200 nm) relative to larger ones (Nakayama et al., 2010; Drinovec et al., 2015). Prior to May 27, the South China Sea region was predominantly influenced by air masses originating from Luzon. The particle size distribution centered a size range of 50-150 nm (Fig. 2a1 in the manuscript), aligning with the particle size distribution of black carbon from urban emissions reported in Schwarz et al. (2008). It implies that the black carbon might distribute at a relatively small particle size range, which could not fully be detected by the AE33, potentially contributing to the discrepancy between the SMPS-derived and ACSM-measured mass concentrations.

Additionally, we analyzed data from another campaign conducted over the South China Sea in June 2022. During this campaign, a typhoon (Chaba) altered local circulation patterns, leading to the transport of substantial pollutants from the Indochinese Peninsula to the ocean after June 28th (Fig. 1.1). Under these conditions, the mass concentrations measured by the SMPS were again consistently higher than those measured by the ACSM (Fig. 1.2), suggesting that the small size black carbon particle could be the primary factor underlying the mass discrepancy.

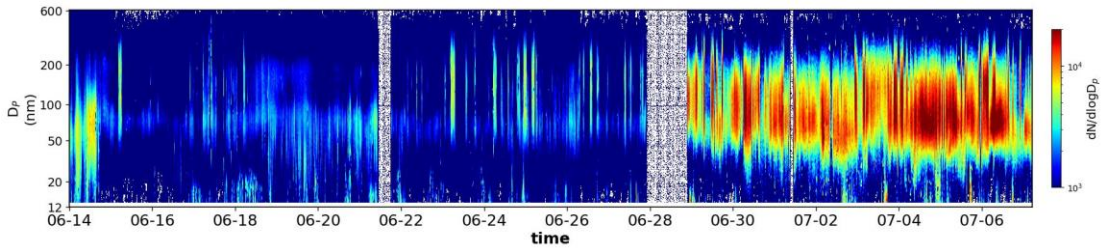

Figure 1.1. Timeseries of particle number size distribution in June 2022 in South China Sea.

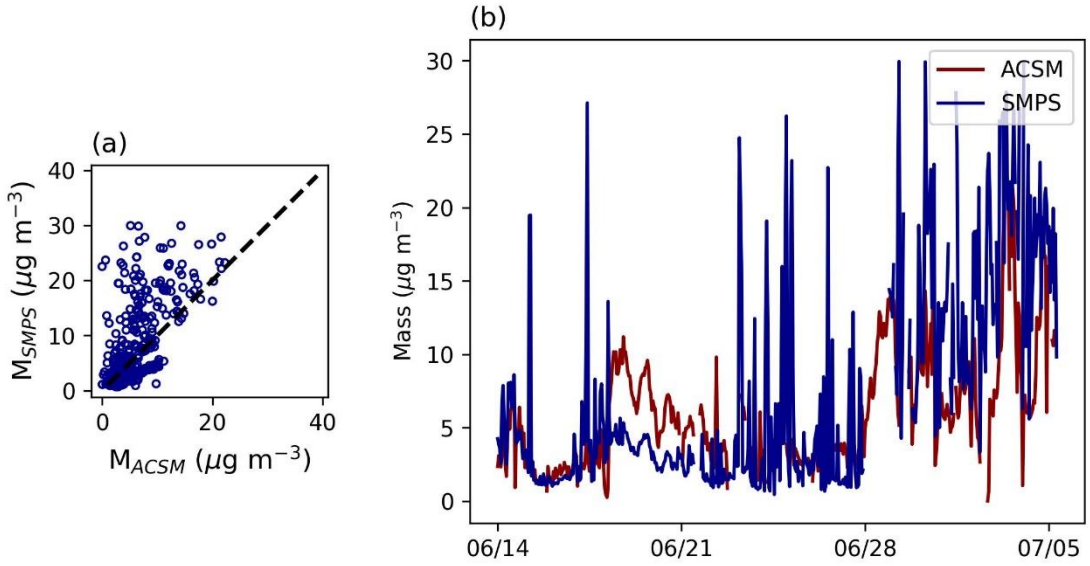

Figure 1.2. Comparison of mass concentration from ACSM and SMPS (a), the timeseries of mass concentration of ACSM and SMPS (b).

A review of the literature indicates that discrepancies between SMPS and AMS/ACSM measurements have been observed at other locations as well (Sun et al., 2016; Wang et al., 2016; Kuang et al., 2020). When a CE of 0.5 was applied, the correlation coefficient for summer slightly increased from 0.84 to 0.85, though the overall difference remained negligible. Additionally, differences in measurement ranges and methodologies between the SMPS and ACSM are likely contributing factors to these discrepancies. We have added the relevant information in lines 191-193 of the manuscript:

Detailed CE calculation and discussion can be found in the supplementary (Text S1, and Fig. S3). Assuming an average aerosol density of 1.5 g cm^{-3} (Geller et al., 2006), the mass concentrations measured by the SMPS and ACSM exhibit a strong overall correlation, with correlation coefficients of 0.84 in summer and 0.93 in winter.

We also have added the discussion in Text S1:

In addition, the SMPS data was used to compared with ACSM data in order to verify the CE value. An average particle density of 1.5 g cm^{-3} was assumed to convert the PNSD data obtained from the SMPS into mass concentrations (Geller et al., 2006). Overall, the mass concentration time series measured by the ACSM and SMPS showed strong correlations, with correlation coefficients of 0.84 and 0.93 for summer and winter, respectively. However, before May 27 (prior to the onset of the

summer monsoon), when air masses predominantly originating from Luzon in the Philippines were observed, SMPS-derived values consistently exceeded those measured by the ACSM. According to Chao et al. (2022), the summer monsoon onset occurred during the sixth pentad of May, which was approximately represented as May 27 for simplicity here. This discrepancy may be attributed to the ACSM's inability to detect certain refractory materials.

To further investigate this discrepancy, we compared black carbon concentrations during two distinct periods, utilizing measurements from the Aethalometer (model AE33). The differences in BC concentration between these periods were minor (0.67 μg m-3 vs 0.48 μg m-3), insufficient to account for the observed discrepancy between the SMPS-derived mass concentration and ACSM mass concentration. It is noteworthy that the AE33 might underestimate BC concentrations during May 5 to 27, owing to the lower detection efficiency for smaller black carbon particles (< 200 nm) relative to larger ones (Nakayama et al., 2010; Drinovec et al., 2015). Prior to May 27, the South China Sea region was predominantly influenced by air masses originating from Luzon. The particle size distribution centered a size range of 50-150 nm (Fig. 2a1 in the manuscript), aligning with the particle size distribution of black carbon from urban emissions reported in Schwarz et al. (2008). It implies that the black carbon might distribute at a relatively small particle size range, which could not fully be detected by the AE33, potentially contributing to the discrepancy between the SMPS-derived and ACSM-measured mass concentrations.

A review of the literature indicates that discrepancies between SMPS and AMS/ACSM measurements have been observed at other locations as well (Sun et al., 2016; Wang et al., 2016; Kuang et al., 2020). When a CE of 0.5 was applied, the correlation coefficient for summer slightly increased from 0.84 to 0.85, though the overall difference remained negligible. Additionally, differences in measurement ranges and methodologies between the SMPS and ACSM are likely contributing factors to these discrepancies.

References:

Drinovec, L., Močnik, G., Zotter, P., Prévôt, A.S.H., Ruckstuhl, C., Coz, E., Rupakheti, M., Sciare, J., Müller, T., Wiedensohler, A., Hansen, A.D.A., 2015. The "dual-spot" Aethalometer: an improved measurement of aerosol black carbon with real-time loading compensation. Atmos. Meas. Tech. 8, 1965-1979.

Geller, M., Biswas, S., Sioutas, C., 2006. Determination of Particle Effective Density in Urban Environments with a Differential Mobility Analyzer and Aerosol Particle Mass Analyzer. Aerosol Sci Tech 40, 709-723.

Kuang, Y., He, Y., Xu, W., Zhao, P., Cheng, Y., Zhao, G., Tao, J., Ma, N., Su, H., Zhang, Y., Sun, J., Cheng, P., Yang, W., Zhang, S., Wu, C., Sun, Y., Zhao, C., 2020. Distinct diurnal variation in organic aerosol hygroscopicity and its relationship with oxygenated organic aerosol. Atmos. Chem. Phys. 20, 865-880.

Nakayama, T., Kondo, Y., Moteki, N., Sahu, L.K., Kinase, T., Kita, K., Matsumi, Y., 2010. Size-dependent correction factors for absorption measurements using filter-based photometers: PSAP and COSMOS. Journal of Aerosol Science 41, 333-343.

Schwarz, J. P., Gao, R. S., Spackman, J. R., Watts, L. A., Thomson, D. S., Fahey, D. W., Ryerson, T. B., Peischl, J., Holloway, J. S., Trainer, M., Frost, G. J., Baynard, T., Lack, D. A., de Gouw, J. A., Warneke, C., and Del Negro, L. A.: Measurement of the mixing state, mass, and optical size of individual black carbon particles in urban and biomass burning emissions, 35, doi:https://doi.org/https://doi.org/10.1029/2008GL033968, 2008.

Sun, Y., Jiang, Q., Xu, Y., Ma, Y., Zhang, Y., Liu, X., Li, W., Wang, F., Li, J., Wang, P., Li, Z., 2016. Aerosol characterization over the North China Plain: Haze life cycle and biomass burning impacts in summer. 121, 2508-2521.
Wang, Q., Zhao, J., Du, W., Ana, G., Wang, Z., Sun, L., Wang, Y., Zhang, F., Li, Z., Ye, X., Sun, Y., 2016. Characterization of submicron aerosols at a suburban site in central China. Atmos Environ. 131, 115-123.

Closure study

Such CCN closure studies have long been conducted. As the authors admit in the manuscript, the ACSM is unable to measure NaCl, leading to some uncertainties in the closure study. I could not understand the reason why calculations for the external mixing case were needed, even if the authors did not show any supporting data about mixing state of aerosol particles.

This manuscript is a measurement report. I personally did not feel that the addition of the closure study enhanced the quality of the manuscript from the perspective of reporting the data. It may make sense to consider deleting the section. If the authors think that the description is critical for the manuscript, it would be needed to add some additional descriptions about the importance and novelty of the closure study.

Reply: Thank you for the reviewer's suggestion. In the previous version, we conducted sensitivity experiments by cross-calculating cloud condensation nuclei (CCN) concentrations using the average D_{50} and PNSD from different seasons to explore which factor—hygroscopicity or PNSD—primarily influences CCN concentrations across seasons. Based on previous reviewer comments and considering that this is a measurement report, we determined that applying the CCN closure method is a more standardized and appropriate approach for brief data analysis, as it effectively links chemical composition with CCN activity. Therefore, we tried to use the CCN closure method for a straightforward interpretation of our data. Although the ACSM does not fully capture the mass concentration of sea salt, its contribution to the overall aerosol mass fraction is not significant (Wu et al., 2022) and has a minor effect on our conclusions. Results from the CCN closure method indicate that summer aerosol and large-sized aerosol in winter predominantly existed in an internally mixed state, while small-sized aerosol in winter was primarily externally mixed. This external mixing state may partly explain the lower hygroscopicity of small-sized particles observed during winter. Thus, we believe that using the CCN closure method to interpret our data is a reasonable approach in this measurement report. We have added some additional descriptions about the importances and novelty of the closure study in lines 452-457:

The CCN closure method is a widely used approach that connects CCN activity with aerosol chemical composition (Cai et al., 2018; Meng et al., 2014; Deng et al., 2013). Studies have demonstrated that the aerosol mixing state is crucial for accurately parameterizing CCN activity (Su et al., 2010; Wang et al., 2010; Ervens et al., 2010). Moreover, the CCN closure method provides a framework for investigating the influence of aerosol mixing states on CCN activity (Padró et al., 2012; Wang et al., 2018; Patel et al., 2021). In this study, we applied two schemes based on the CCN closure method, as described in Section 2.2.3, which consider aerosol composition and mixing state.

References:

Wu, C.-H., Yuan, C.-S., Yen, P.-H., Yeh, M.-J., Soong, K.-Y., 2022. Diurnal and seasonal variation,

chemical characteristics, and source identification of marine fine particles at two remote islands in South China Sea: A superimposition effect of local emissions and long-range transport. Atmos Environ. 270, 118889.

We sincerely appreciate the reviewers for taking the time to review our manuscript and for providing valuable comments. Based on the reviewers' suggestions, we have revised the paper. Below are our responses to each of the reviewers' comments, with the reviewers' comments in black, our responses in red, and the revised manuscript content in italicized orange font.

Reviewer 2

This manuscript presents a comprehensive aerosol and CCN properties over the South China Sea (SCS) during summer and winter from two ship-based measurements. The aerosol size distribution, chemical composition of PM_1, hygroscopicity, and the CCN (with closure study) are examined and briefly analyzed, and the seasonal variations in the aerosol species and activation ratio is evident. This study provides extra data sources for future studies over the SCS. I think this manuscript holds the potential of publication, after considering and addressing the concerns and questions I have listed below.

We sincerely thank the reviewer for their valuable and insightful comments, which have significantly improved the quality of our manuscript. In response, we have included additional measurement-related information, addressed critical details that were previously omitted in certain sections, and revised and supplemented relevant figures and tables to enhance the clarity and coherence of our presentation.

Measurements

1. Please specify the instruments (CCN counter, SMPS, and DMA), measurable size range (and bin size if applicable), frequency, and instrumental uncertainty on the size-resolved number concentrations.

Reply: Thank you for the reviewer's valuable suggestions. The Scanning Mobility Particle Sizer (SMPS) comprises a Differential Mobility Analyzer (DMA) and a Condensation Particle Counter (CPC). In the Scanning Mobility CCN Analysis (SMCA) method, the SMPS is integrated with the CCN counter (CCNc). After particle size selection by the DMA, particles are directed simultaneously to both the CPC and the CCNc, so we did not need a separate DMA.

The DMA scanning ranges used in the SMPS during the two campaigns are specified in lines 160-161 of the manuscript: 10–500 nm for the summer campaign and 10–593 nm for the winter campaign. The CCNc operated with a scanning duration of 20 minutes for each supersaturation level, while the DMA completed a full particle size scanning cycle every 5 minutes. This additional detail has been included in lines 170-171 of the manuscript:

During the measurement process, each supersaturation level was held constant for 20 minutes, with the DMA completing a full scanning cycle every 5 minutes.

The uncertainty in the instrument's measurement of size-resolved particle number concentration is approximately 5%-6% (Morre et al. 2010) and we have included this information in lines 178-179:

The uncertainty in the instrument's measurement of size-resolved particle number concentration is approximately 5%-6% (Morre et al. 2010).

2. What is the supersaturation ramping time scale for the CCN column A?

Reply: Thanks for reviewer's question. During the measurements, supersaturation varied from 0.1% to 0.2%, 0.2% to 0.4%, and 0.4% to 0.7%, with temperature stabilization times ranging from a few seconds to tens of seconds. However, transitioning from 0.7% to 0.1% or 0.2% required approximately 5 minutes. In data processing, only cases where temperature remained stable during

the DMA scanning phase were selected. We have added the supersaturation ramping time scale on lines 171-176:

During the measurement process, each supersaturation level was held constant for 20 minutes, with the DMA completing a full scanning cycle every 5 minutes. During the measurements, supersaturation levels varied incrementally between 0.1% and 0.2%, 0.2% and 0.4%, and 0.4% and 0.7%, with temperature stabilization times ranging from a few seconds to several tens of seconds. However, reducing the supersaturation from 0.7% to 0.1% or 0.2% required approximately 5 minutes for stabilization. For data processing, only instances where the temperature remained stable throughout the DMA scanning phase were included in the analysis.

3. Also, the error or precision of the ACSM measured mass concentration should be specified after the composition-dependent collection efficiency correction.

Reply: Thanks for reviewer's comment. The values obtained using the time-independent CE method deviate by approximately 3% compared to those derived with a constant CE of 0.5. We have included this information in lines 191-193:

The values obtained using the time-independent CE method show a deviation of approximately 3% compared to those obtained with a constant CE of 0.5.

4. The uncertainties for the meteorological quantities need to be reported.

Reply: Thanks for reviewer's suggestion. The automatic weather stations on the Jiageng and Sun Yat-sen research vessels were manufactured by the Finnish company Vaisala, with model numbers AWS430 and WXT536, respectively. The AWS430 provides measurement accuracies of ±2% for wind speed, ±2% for wind direction, ±0.3°C for temperature, and ±1% for relative humidity (within the range of 0–90%). Similarly, the WXT536 offers accuracies of ±3% for wind speed, ±3% for wind direction, ±0.3°C for temperature, and ±3% for relative humidity (within the range of 0–90%) (http://www.vaisala.com). We have added their accuracy specifications in lines 202–210 of the revised manuscript:

The meteorological elements, including temperature, relative humility (RH), wind speed, and wind direction, were measured by the combined automatic weather station (AWS430, Vaisala Inc., Finland) onboard the vessels (Sun et al., 2024). During the winter cruises, meteorology data before 12.22 was missed due to the calibration for the automatic weather station (WXT536, Vaisala Inc., Finland) before 12.22. The timeseries of meteorological data were presented in Fig. S4. The AWS430 provides measurement accuracies of ±2% for wind speed, ±2% for wind direction, ±0.3 ℃ for temperature, and ±1% for relative humidity (within the range of 0–90%). Similarly, the WXT536 offers accuracies of ±3% for wind speed, ±3% for wind direction, ±0.3 ℃ for temperature, and ±3% for relative humidity (within the range of 0–90%) (www.vaisala.com).

5. More details on the aethalometer are also encouraged (size ranges, uncertainty, etc.).

Reply: Thanks for reviewer's suggestion. The AE33 measures the black carbon (BC) mass concentration in $PM_{2.5}$. These concentrations are referred to as equivalent BC mass concentrations because they represent the light absorption of BC at a wavelength of 880 nm. We have incorporated the relevant details about the AE33 in lines 195–200 of the manuscript:

The black carbon (BC) mass concentrations were measured using an aethalometer (Model AE33, Magee Scientific, USA) with a 1-minute time resolution (Drinovec et al., 2015). Notably, the BC

mass concentrations obtained from AE33 are referred to as equivalent BC mass concentrations, as they represent the combined light absorption of BC at 880 nm. Prior to entering the AE33, the sampled air was passed through a $PM_{2.5}$ cyclone (BGI Inc., Waltham, MA, USA) to exclude particles larger than 2.5 μm.

6. In the CCN closure section, can you report representative D50 values for four species (as in S7) under the External scheme, during summer and winter seasons in the study domain?
Reply: We have reported the D50 calculated by Eq. (2) according to the hygroscopicity of different species in Table S1. We have included the information in lines 275-279:
(2) External-mixed scheme: the aerosol composition from the ToF-ACSM was assumed to be size-independent and externally mixed. Four type of aerosol ($(NH_4)_2SO_4$, NH_4NO_3, NaCl and organic) are assumed to have a same proportion for all sizes. The D50 from each species was calculated by Eq. (2) according to their κ values mentioned in 2.2.2. N_{CCN} is calculated according to the Eq. (5) (Fig. S8b and Table S1).

D_{50} (nm)	0.1% SS	0.2% SS	0.4% SS	0.7% SS
Sulfate	143	90	57	39
Seasalt	109	69	43	30
Nitrate	135	85	53	37
Organic	242	192	152	126

Table S1. The D_{50} of different species in external scheme.

I believe those are crucial for a measurement report.

Specific Comments:
Line 117: Can you elaborate on how the seasonal variation of the fraction of high cloud is relevant here in terms of the ship-observed CCN near the sea surface and the aerosol-high cloud interaction? Intuitively, would the lower boundary layer aerosol/CCN have greater impacts on the MBL clouds, or is there any particular dynamical mechanism the author is referring to?
Reply: Thanks for reviewer's comment. Given the absence of a well-established mechanism linking boundary layer aerosol properties and cloud condensation nuclei concentrations to the formation of high-altitude clouds, we revised the sentence to enhance clarity and cited new references that specifically discuss the influence of boundary layer aerosol variations on cumulus cloud properties over the South China Sea (Lines 119-122):
Additionally, when the marine boundary layer over the SCS is influenced by various natural and anthropogenic sources, resulting in altered aerosol properties, the characteristics of cumulus clouds are correspondingly affected (Miller et al., 2023). This indicates that aerosol-cloud interactions vary between winter and summer seasons.

L153. 'The ··· SMCA··· was initially···'. And do you want to say you utilize this sampling strategy to get the size-resolved CCN?
Reply: Thanks for the reviewer's valuable comment. We apologize for the lack of clarity in the original sentence. What we intended to convey is: The size-resolved CCN activity was measured using the scanning mobility CCN analysis (SMCA) method proposed by Moore et al. (2010), employing a combination of a scanning mobility particle sizer (SMPS) system and a cloud

condensation nuclei counter (CCNc-200, DMT Inc., USA). We have revised the sentence accordingly (Lines 155-157):

The size-resolved CCN activity was measured using the scanning mobility CCN analysis (SMCA) method proposed by Moore et al. (2010), employing a combination of a scanning mobility particle sizer (SMPS) system and a cloud condensation nuclei counter (CCNc-200, DMT Inc., USA) (Fig. S2).

L159. Have both sensors in the counter column B on two ships malfunctioned during the two sampling periods?

Reply: Thanks for reviewer's comment. Column B in CCNc was not used on both cruises. We have added the information in lines 161-162:

Unfortunately, due to the malfunction of flow sensor in the column B on both cruises, only the data from column A is presented in this study.

L206. You have introduced D50 as 'particle size at which 50% of the particles are activated at a specific SS' before. Your statement here is flawed.

Reply: Thank you for the reviewer's valuable feedback. We apologize for the error and have corrected this statement (Line 230):

Additionally, it is noting that the estimated κ values refer to particles with the D_{50}.

L275. The results in S8 and S9 are well-justified, though, you should consider putting a few words about it in the main text.

Reply: Thanks for reviewer's comment. We have added some words about the Figure S8 (Lines 314-316):

Minor discrepancies may exist between the air mass origins at certain midpoints and the actual ship locations. However, overall, the air mass origins at the midpoints are representative of those at the actual locations.

L307. Winter period shows two peaks with more organic (less sulfate) and with both high organic and sulfate. Elaborate on how the impact of Northeast Monsoon 'persist'.

Reply: Thank you for the reviewer's comments. During the winter cruise, the winter monsoon was already dominant. The presence of two distinct peaks suggests that the two phases were likely influenced by air masses from different sources. As discussed later, the "Mainland China" phase exhibited a higher proportion of organic matter, while both sulfate and organic matter were relatively elevated during the "Mixed" phase.

L311. Define clearly how the Nucleation, Aikten, and Accumulation are defined, in terms of size cut and rationale, in this study (should have been done in the Data section).

Reply: Thanks for reviewer's comment. The Nucleation mode, Aikten, and Accumulation are defined by their geometric mean diameters (GMD). The GMD for nucleation modes (GMD1) typically ranges from 3 to 30 nm, for Aitken modes (GMD2) from 30 to 100 nm, and for accumulation modes (GMD3) above 100 nm. We have added a section in the Data section to describe the three modes (Section 2.2.4, lines 284-298):

The multi-lognormal distribution function (Eq. (8)) is used to parameterize and optimize the descriptions of the measured PNSD (Heintzenberg, 1994) and is widely applied in aerosol research (Cai et al, 2020; Boyer et al., 2023; Zhu and Wang, 2024). An automatic mode-fitting algorithm (Hussein et al., 2005) is used to generate the model-fitted results.

$$f\left(D_p, \bar{D}_{pg,i}, N_i, \sigma_{g,i}\right) = \sum_{i=1}^{n} \frac{N_i}{\sqrt{2\pi}\log(\sigma_{g,i})} \times exp\left[-\frac{\left[\log D_p - \log \bar{D}_{pg,i}\right]^2}{2\left(\log \sigma_{g,i}\right)^2}\right] \quad (8)$$

where D_P is the diameter of a particle. Each lognormal mode is characterized by three parameters: the mode number concentration (N_i), geometric variance ($\sigma_{g,i}$), and geometric mean diameter (GMD, $\bar{D}_{pg,i}$). The total number of lognormal modes used to describe the PNSD is denoted by n. These modes are fitted using an algorithm applied to each particle size distribution, with one to three log-normal distributions used per time step. The algorithm classifies the PNSD into nucleation, Aitken, and accumulation modes based on their geometric mean diameters (GMDs). The GMD for nucleation modes (GMD1) typically ranges from 3 to 30 nm, for Aitken modes (GMD2) from 30 to 100 nm, and for accumulation modes (GMD3) above 100 nm (Heintzenberg, 1994; Hussein et al., 2005; Zhu and Wang, 2024).

L330. Explanation is needed on the flipped hygroscopicity-supersuration relations between summer and winter.

Reply: Thanks for reviewer's comment. We have explained the possible reason in lines 379-384:

This contrasting trend may be related to the reduced sulfate fraction in smaller sizes during winter, as sulfate production via DMS oxidation is diminished due to lower sea surface temperatures in winter (18.0 ℃) compared to summer (29.3 ℃), which in turn inhibits DMS production by phytoplankton (Bates et al., 1987; Kouvarakis and Mihalopoulos, 2002). Additionally, it could be linked to the mixing state of the particles, with further discussion provided in the following sections.

L388. Which figure or table are you referring to wrt. 'smaller sizes'. And yes, sulfate fraction is reduced in winter 'Marine' period, but the increased ammonium may compensate for this effect (Fig. 5f). You may also consider attributing this to the increases in organic aerosol contribution due to factors like reduced photochemical oxidation.

Reply: Thank you for the reviewer's comment. The smaller sizes refer to hygroscopicity at high supersaturation (0.7% SS), since the D_{50} at high SS was much lower than those at low SS. We have included this information in lines 233-235:

According to κ-Köhler theory, in the following discussion, the hygroscopicity of small particles is associated with hygroscopicity at high SS, whereas the hygroscopicity of large particles is linked to hygroscopicity at low SS.

We modified the sentence in L388 (in previous version) to clarify:

Additionally, as discussed in Section 3.1, the reduced biological activity during winter, which results in a decline in the fraction of small-particle sulfate and an increase in the fraction of organics, may also contribute to this low hygroscopicity in small particles (at high SS, fig 7b).

We also consider that the higher fraction of organic aerosols at smaller sizes, resulting from the lower sulfate concentrations due to reduced biological activity in winter, may contribute to the lower hygroscopicity at high SS. We have added the relevant information in lines 437-441:

This suggests that the lower hygroscopicity in smaller particles during the "Mainland China" period may be attributed to a larger fraction of hydrophobic BC. Additionally, as discussed in Section 3.1, the reduced biological activity during winter, which results in a decline in the fraction of small-particle sulfate and an increase in the fraction of organics, may also contribute to this low hygroscopicity in small particles.

Technical comments:

L56. '…partially attributed…'. And considering adding more recent and relevant references to these statements.

Reply: We have corrected the word and added more references.

L71. Please be more specific on what particles (compositions, sizes, etc.) were examined in Ajith et al. (2022)

Reply: In Ajith et al. (2022), "particles" refer to total particles without specifying any particle type or size range. According to Köhler theory, only small particles are considered in discussions about their activation as cloud condensation nuclei (CCN), whereas larger particles can act as CCN directly.

L90. This paper (Zheng et al., 2020) is not on the reference list. And I presume you refer to 'Eastern North Atlantic'.

Reply: Thanks for reviewer's comments. We have added the reference and corrected the location to "Eastern North Atlantic".

L153. 'The … SMCA… was initially…'.

Reply: We have corrected the word.

L153. '(Fig. 1c2)'

Reply: We consider that we can reference Figure S2 here.

L377. Here, the statement, though reasonable, has not been supported by the results, use 'potentially led' instead.

Reply: We have corrected the word.

Figures. Please put the figure caption directly beneath the figure.

Reply: We have put the figure caption beneath the figure.

Fig. 3. Same y-axis range is needed for (a) and (b). And please state the seasons for (e) and (f).

Reply: We have redrawn Figure 3.

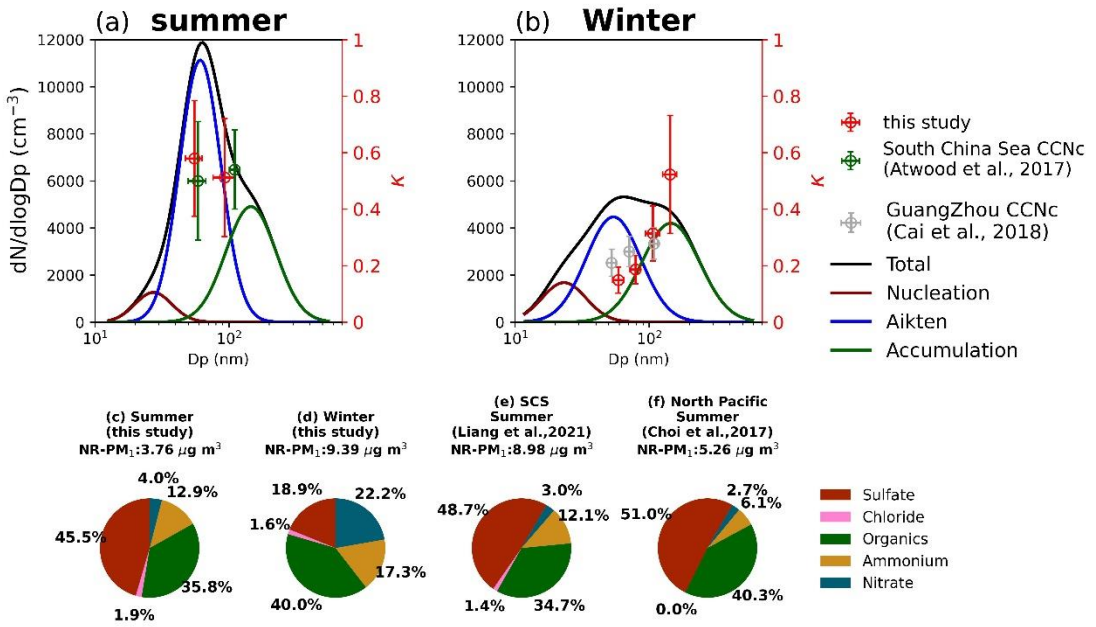

Figure 3. Particle number size distribution in summer (a) and winter (b); The red markers represent the activation diameters and hygroscopicity parameters corresponding to 0.1%, 0.2%, 0.4%, and 0.7% supersaturations in this study (without 0.1% in summer). The green markers represent the hygroscopicity parameters reported in Atwood et al. (2017) for the southern South China Sea during summer. The gray markers represent the hygroscopicity parameters documented in Cai et al. (2018) for the Pearl River Delta region during winter. The fraction of NR-PM1 in summer (c) and winter (d) in this study, in northern SCS reported by Liang et al. (2021) (e), and in North Pacific reported by Choi et al. (2017) (f).

Fig. S9. Panel (c) and (f), consider using something like 'Marine-Win'? I was confused with Marine-(South) and Marine-(West) at first glance.

Reply: We have redrawn the Figure S10 (Original Fig. S9).

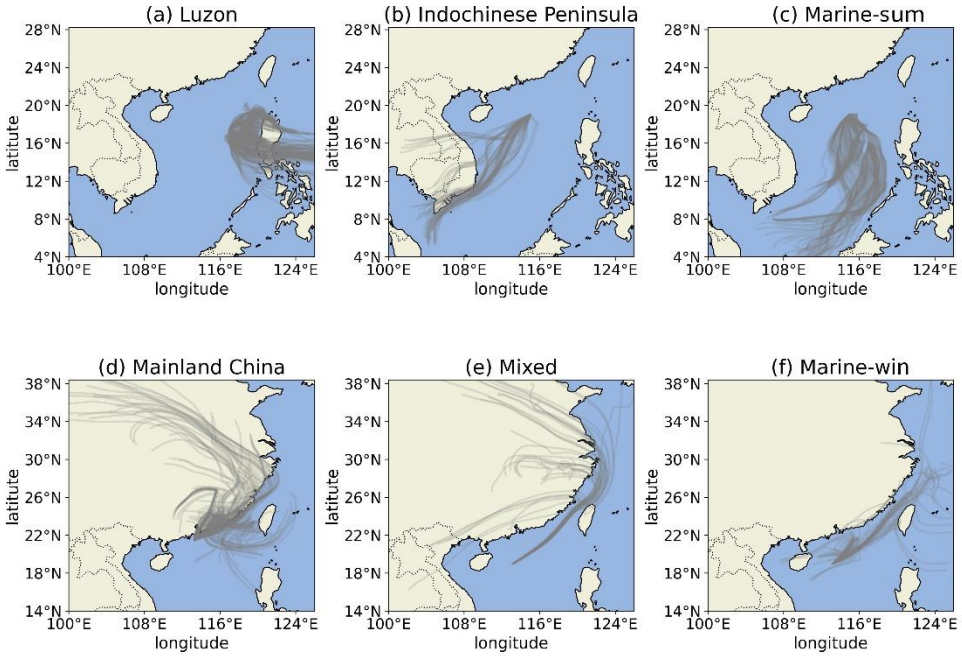

Figure S10. The backward trajectories of different clusters in summer (a) and winter (b).

Fig. S14. Use more distinguishable colors between 14.6 and 41.4 nm. And the subpanel labels do not match the captions for winter.

Reply: We have redrawn the Figure 15 (Original Fig. S14):

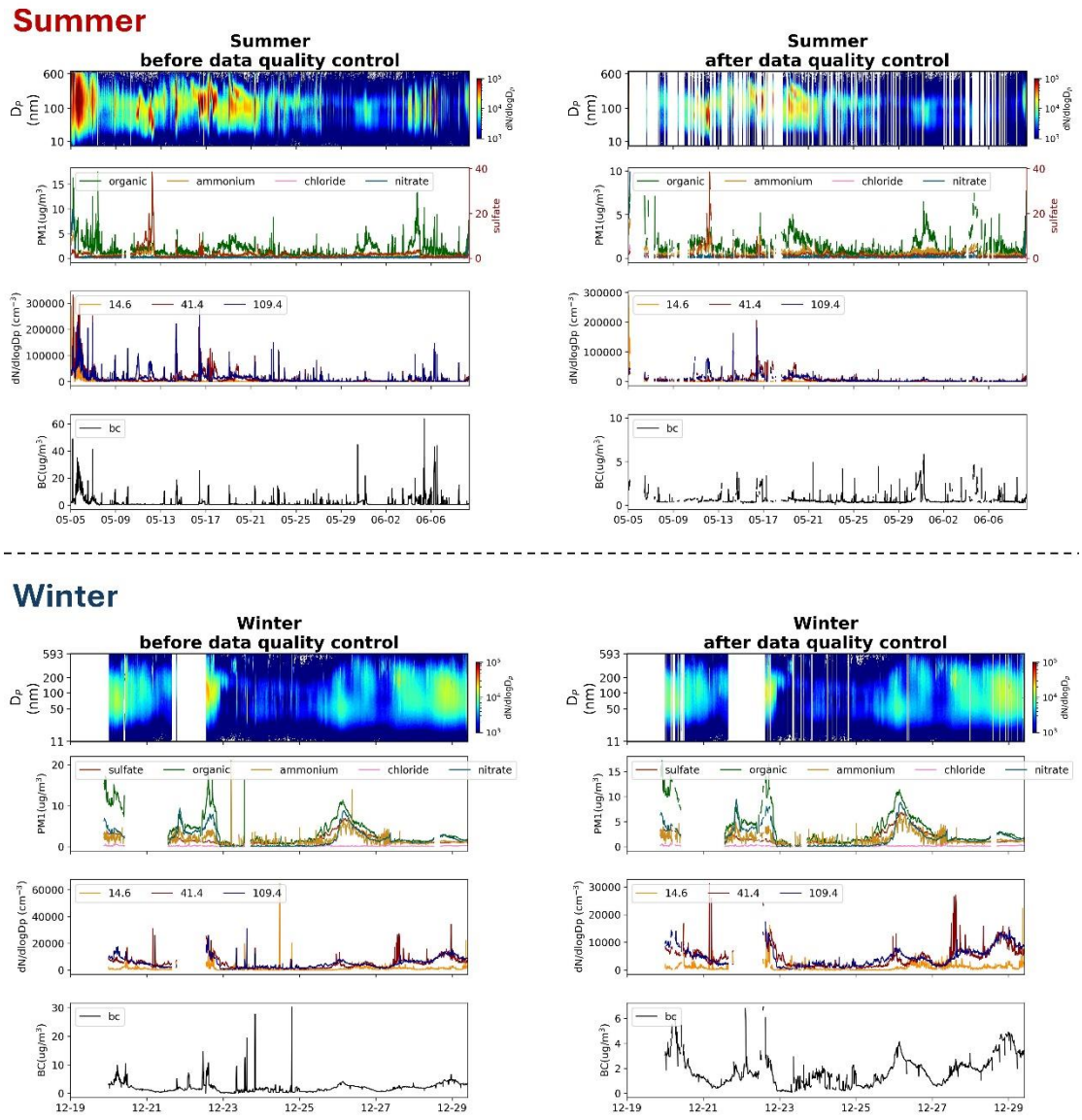

Figure S15. Timeseries of particle number size distribution (a) and (e), mass concentration of NR-PM1 (b) and (f), particle number concentration in 14.6, 41.4, and 109.4 nm (c) and (g), mass concentration of black carbon (d) and (h); The figure number from (a) to (d) means the data in summer, and the figure nnmber from (e) to (h) means the data in winter; The number 1 represented the data before data quality control and the number 2 represent the data after data quality control.

Reference. The reference list is hard to distinguish between entries, so please correct the format.

Reply: We have changed the format on the reference list to make it clear.